References

1. Berger H (1929) Arch Psychiat 87: 527.
2. Steriade M (2001) Impact of network activities on neuronal properties in corticothalamic systems. J Neurophysiol 86: 1-39.
3. Palva S, Palva JM (2007) New vistas for alpha-frequency band oscillations. Trends Neurosci 30: 150-158.
4. Vecchiato G, Astolfi L, De Vico Fallani F, Toppi J, Aloise F, et al. (2011) On the use of EEG or MEG brain imaging tools in neuromarketing research. Computational intelligence and neuroscience 2011: 643489.
5. Vecchiato G, Toppi J, Astolfi L, De Vico Fallani F, Cincotti F, et al. (2011) Spectral EEG frontal asymmetries correlate with the experienced pleasantness of TV commercial advertisements. Medical & biological engineering & computing 49: 579-583.
6. Astolfi L, De Vico Fallani F, Cincotti F, Mattia D, Bianchi L, et al. (2008) Neural basis for brain responses to TV commercials: a high-resolution EEG study. IEEE transactions on neural systems and rehabilitation engineering : a publication of the IEEE Engineering in Medicine and Biology Society 16: 522-531.
7. Sadato N, Nakamura S, Oohashi T, Nishina E, Fuwamoto Y, et al. (1998) Neural networks for generation and suppression of alpha rhythm: a PET study. Neuroreport 9: 893-897.
8. Lindgren KA, Larson CL, Schaefer SM, Abercrombie HC, Ward RT, et al. (1999) Thalamic metabolic rate predicts EEG alpha power in healthy control subjects but not in depressed patients. Biol Psychiatry 45: 943-952.
9. Larson CL, Davidson RJ, Abercrombie HC, Ward RT, Schaefer SM, et al. (1998) Relations between PET-derived measures of thalamic glucose metabolism and EEG alpha power. Psychophysiology 35: 162-169.
10. Oohashi T, Nishina E, Honda M, Yonekura Y, Fuwamoto Y, et al. (2000) Inaudible high-frequency sounds affect brain activity: hypersonic effect. Journal of neurophysiology 83: 3548-3558.
11. Goldman RI, Stern JM, Engel J, Jr., Cohen MS (2002) Simultaneous EEG and fMRI of the alpha rhythm. Neuroreport 13: 2487-2492.
12. Moosmann M, Ritter P, Krastel I, Brink A, Thees S, et al. (2003) Correlates of alpha rhythm in functional magnetic resonance imaging and near infrared spectroscopy. Neuroimage 20: 145-158.
13. Laufs H, Kleinschmidt A, Beyerle A, Eger E, Salek-Haddadi A, et al. (2003) EEG-correlated fMRI of human alpha activity. Neuroimage 19: 1463-1476.
14. Laufs H, Holt JL, Elfont R, Krams M, Paul JS, et al. (2006) Where the BOLD signal goes when alpha EEG leaves. Neuroimage 31: 1408-1418.

15. Goncalves SI, de Munck JC, Pouwels PJ, Schoonhoven R, Kuijer JP, et al. (2006) Correlating the alpha rhythm to BOLD using simultaneous EEG/fMRI: inter-subject variability. Neuroimage 30: 203-213.

16. Difrancesco MW, Holland SK, Szaflarski JP (2008) Simultaneous EEG/functional magnetic resonance imaging at 4 Tesla: correlates of brain activity to spontaneous alpha rhythm during relaxation. J Clin Neurophysiol 25: 255-264.

17. Tyvaert L, Levan P, Grova C, Dubeau F, Gotman J (2008) Effects of fluctuating physiological rhythms during prolonged EEG-fMRI studies. Clin Neurophysiol 119: 2762-2774.

18. Nikouline VV, Linkenkaer-Hansen K, Wikstrom H, Kesaniemi M, Antonova EV, et al. (2000) Dynamics of mu-rhythm suppression caused by median nerve stimulation: a magnetoencephalographic study in human subjects. Neuroscience letters 294: 163-166.

19. Wolpaw JR, McFarland DJ (2004) Control of a two-dimensional movement signal by a noninvasive brain-computer interface in humans. Proc Natl Acad Sci U S A 101: 17849-17854.

20. de Munck JC, Goncalves SI, Huijboom L, Kuijer JP, Pouwels PJ, et al. (2007) The hemodynamic response of the alpha rhythm: an EEG/fMRI study. Neuroimage 35: 1142-1151.

21. de Munck JC, Goncalves SI, Mammoliti R, Heethaar RM, Lopes da Silva FH (2009) Interactions between different EEG frequency bands and their effect on alpha-fMRI correlations. Neuroimage 47: 69-76.

22. Salek-Haddadi A, Friston KJ, Lemieux L, Fish DR (2003) Studying spontaneous EEG activity with fMRI. Brain Res Brain Res Rev 43: 110-133.

23. Niedermeyer E, da Silva FL (2004) Electroencephalography: basic principles, clinical applications, and related fields.

24. Rechtschaffen A, Kales A (1986) A manual of standardized terminology, techniques and scoring system for sleep stages of human subjects. Washington DC: US Public Health Service, US Government Printing Office.

25. Huang NE, Shen Z, Long SR, Wu MLC, Shih HH, et al. (1998) The empirical mode decomposition and the Hilbert spectrum for nonlinear and non-stationary time series analysis. Proceedings of the Royal Society of London Series a-Mathematical Physical and Engineering Sciences 454: 903-995.

26. Bear MF, Connors BW, Paradiso MA (2007) Neuroscience : exploring the brain. Philadelphia, PA: Lippincott Williams & Wilkins. xxxviii, 857 p. p.

27. Laufs H, Daunizeau J, Carmichael DW, Kleinschmidt A (2008) Recent advances in recording electrophysiological data simultaneously with magnetic resonance imaging. Neuroimage 40: 515-528.

28. Allen PJ, Polizzi G, Krakow K, Fish DR, Lemieux L (1998) Identification of EEG events in the MR scanner: the problem of pulse artifact and a method for its subtraction. Neuroimage 8: 229-239.

29. Allen PJ, Josephs O, Turner R (2000) A method for removing imaging artifact from continuous EEG recorded during functional MRI. Neuroimage 12: 230-239.

30. Hyvarinen A, Karhunen J, Oja E (2001) Independent component analysis. New York: J. Wiley. xxi, 481 p. p.

31. Makeig S, Bell AJ, Jung TP, Sejnowski TJ (1996) Independent Component Analysis of Electroencephalographic Data. Cambridge MA: Advances in Neural Information Processing systems, MIT Press.

32. Grouiller F, Vercueil L, Krainik A, Segebarth C, Kahane P, et al. (2007) A comparative study of different artefact removal algorithms for EEG signals acquired during functional MRI. Neuroimage 38: 124-137.

33. Henning S, Merboldt KD, Frahm J (2006) Task- and EEG-correlated analyses of BOLD MRI responses to eyes opening and closing. Brain Res 1073-1074: 359-364.

34. Niazy RK, Xie J, Miller K, Beckmann CF, Smith SM (2011) Spectral characteristics of resting state networks. Progress in brain research 193: 259-276.

35. Rilling G, Flandrin, P., & Gonçalvés, P. (2003) On empirical mode decomposition and its algorithms. IEEE-EURASIP workshop on Nonlinear Signal and Image Processing, NSIP-03, Grado (I).

36. Huang NE, Wu MLC, Long SR, Shen SSP, Qu WD, et al. (2003) A confidence limit for the empirical mode decomposition and Hilbert spectral analysis. Proceedings of the Royal Society of London Series a-Mathematical Physical and Engineering Sciences 459: 2317-2345.

37. Friston KJ, Ashburner JT, Kiebel SJ, Nichols TE, Penny WE (2007) Statistical Parametric Mapping: the analysis of functional brain images. . London, UK: Academic Press, Elsevier. .

38. Schroth G, Klose U (1992) Cerebrospinal fluid flow. III. Pathological cerebrospinal fluid pulsations. Neuroradiology 35: 16-24.

39. Schroth G, Klose U (1992) Cerebrospinal fluid flow. II. Physiology of respiration-related pulsations. Neuroradiology 35: 10-15.

40. Schroth G, Klose U (1992) Cerebrospinal fluid flow. I. Physiology of cardiac-related pulsation. Neuroradiology 35: 1-9.

41. Frackowiak RS (2003) Human brain function: Academic Press.

42. Mai JK, Paxinos G, Voss T (2008) Atlas of the human brain. Amsterdam ; Boston: Elsevier Academic Press.

43. Andersen P, Andersson SA, Lomo T (1967) Some factors involved in the thalamic control of spontaneous barbiturate spindles. J Physiol 192: 257-281.

44. Horovitz SG, Fukunaga M, de Zwart JA, van Gelderen P, Fulton SC, et al. (2008) Low frequency BOLD fluctuations during resting wakefulness and light sleep: a simultaneous EEG-fMRI study. Human Brain Mapping 29: 671-682.

45. Fuxe K, Dahlstrom AB, Jonsson G, Marcellino D, Guescini M, et al. (2010) The discovery of central

monoamine neurons gave volume transmission to the wired brain. Progress in neurobiology 90: 82-100.

46. Steriade M (2006) Grouping of brain rhythms in corticothalamic systems. Neuroscience 137: 1087-1106.
47. Kobayashi H, Libet B (1970) Actions of noradrenaline and acetylcholine on sympathetic ganglion cells. J Physiol 208: 353-372.
48. Akasu T, Gallagher JP, Koketsu K, Shinnick-Gallagher P (1984) Slow excitatory post-synaptic currents in bull-frog sympathetic neurones. J Physiol 351: 583-593.
49. Dun NJ, Kiraly M, Ma RC (1984) Evidence for a serotonin-mediated slow excitatory potential in the guinea-pig coeliac ganglia. J Physiol 351: 61-76.
50. Wallis DI, Dun NJ (1988) A comparison of fast and slow depolarizations evoked by 5-HT in guinea-pig coeliac ganglion cells in vitro. Br J Pharmacol 93: 110-120.
51. Libet B (1992) Introduction to slow synaptic potentials and their neuromodulation by dopamine. Can J Physiol Pharmacol 70 Suppl: S3-11.
52. Naidich TP, Duvernoy HM (2009) Duvernoy's atlas of the human brain stem and cerebellum : high-field MRI : surface anatomy, internal structure, vascularization and 3D sectional anatomy. Wien ; New York: Springer. xi, 876 p. p.
53. Michelsen KA, Prickaerts J, Steinbusch HW (2008) The dorsal raphe nucleus and serotonin: implications for neuroplasticity linked to major depression and Alzheimer's disease. Progress in brain research 172: 233-264.
54. Nieuwenhuys R, Voogd J, Huijzen Cv (2008) The human central nervous system. New York: Springer. xiv, 967 p. p.
55. Schreckenberger M, Lange-Asschenfeldt C, Lochmann M, Mann K, Siessmeier T, et al. (2004) The thalamus as the generator and modulator of EEG alpha rhythm: a combined PET/EEG study with lorazepam challenge in humans. Neuroimage 22: 637-644.
56. Behrens TE, Johansen-Berg H, Woolrich MW, Smith SM, Wheeler-Kingshott CA, et al. (2003) Non-invasive mapping of connections between human thalamus and cortex using diffusion imaging. Nature neuroscience 6: 750-757.
57. Herrero MT, Barcia C, Navarro JM (2002) Functional anatomy of thalamus and basal ganglia. Child's nervous system : ChNS : official journal of the International Society for Pediatric Neurosurgery 18: 386-404.
58. Klein JC, Rushworth MF, Behrens TE, Mackay CE, de Crespigny AJ, et al. (2010) Topography of connections between human prefrontal cortex and mediodorsal thalamus studied with diffusion tractography. Neuroimage 51: 555-564.
59. Hsu MM, Kung JC, Shyu BC (2000) Evoked responses of the anterior cingulate cortex to stimulation of the medial thalamus. The Chinese journal of physiology 43: 81-89.

60. Hsu MM, Shyu BC (1997) Electrophysiological study of the connection between medial thalamus and anterior cingulate cortex in the rat. Neuroreport 8: 2701-2707.

61. Bush G, Luu P, Posner MI (2000) Cognitive and emotional influences in anterior cingulate cortex. Trends in cognitive sciences 4: 215-222.

62. Bush G, Vogt BA, Holmes J, Dale AM, Greve D, et al. (2002) Dorsal anterior cingulate cortex: a role in reward-based decision making. Proceedings of the National Academy of Sciences of the United States of America 99: 523-528.

63. Patel P, Al-Dayeh L, Singh M (1997) Localisation of alpha activity by simultaneous fMRI and EEG measurements. Proc Int Soc Magn Res Med 3: 1653.

64. Fox MD, Raichle ME (2007) Spontaneous fluctuations in brain activity observed with functional magnetic resonance imaging. Nat Rev Neurosci 8: 700-711.

65. Fox MD, Snyder AZ, Vincent JL, Corbetta M, Van Essen DC, et al. (2005) The human brain is intrinsically organized into dynamic, anticorrelated functional networks. Proc Natl Acad Sci U S A 102: 9673-9678.

66. Greicius MD, Krasnow B, Reiss AL, Menon V (2003) Functional connectivity in the resting brain: a network analysis of the default mode hypothesis. Proc Natl Acad Sci U S A 100: 253-258.

67. Raichle ME, MacLeod AM, Snyder AZ, Powers WJ, Gusnard DA, et al. (2001) A default mode of brain function. Proc Natl Acad Sci U S A 98: 676-682.

68. Rogers BP, Morgan VL, Newton AT, Gore JC (2007) Assessing functional connectivity in the human brain by fMRI. Magn Reson Imaging 25: 1347-1357.

69. Bridwell DA, Wu L, Eichele T, Calhoun VD (2013) The spatiospectral characterization of brain networks: Fusing concurrent EEG spectra and fMRI maps. Neuroimage 69: 101-111.

70. Brookes MJ, Hale JR, Zumer JM, Stevenson CM, Francis ST, et al. (2011) Measuring functional connectivity using MEG: methodology and comparison with fcMRI. Neuroimage 56: 1082-1104.

71. He BJ, Snyder AZ, Zempel JM, Smyth MD, Raichle ME (2008) Electrophysiological correlates of the brain's intrinsic large-scale functional architecture. Proceedings of the National Academy of Sciences of the United States of America 105: 16039-16044.

Figure legends

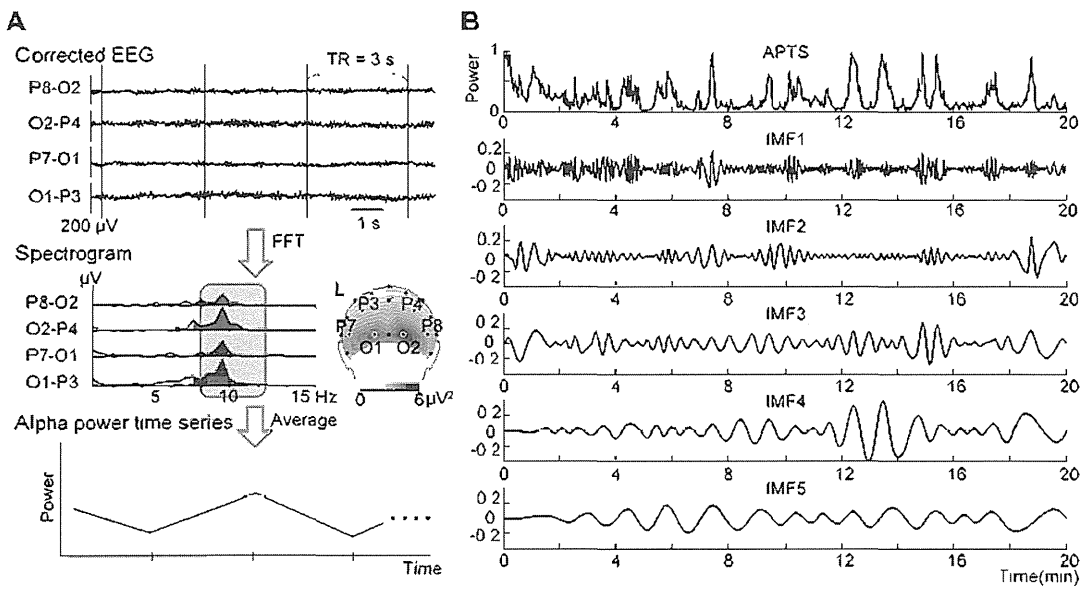

Figure 1. Calculation of the EEG alpha power time series (APTS) and intrinsic mode functions (IMFs). A: After removal of the MRI and ballistocardiogram artifacts, the EEG data from the four bipolar channels were subjected to frequency analysis using fast Fourier transform (FFT) for each 3-second segment (gray in the upper panel). The powers of the alpha band across the four bipolar channels were averaged. The averaged power values were then temporally aligned as the APTS, as shown in the bottom panel. A scalp topography of alpha power of a single subject is shown in the right middle panel. Note that the topography is described by EEG data of a unipolar induction, and L indicates the left side of the brain. B: An example of the IMFs for a single subject. An APTS of a single subject is shown in the upper panel. Next, the IMFs separated by the empirical mode decomposition (EMD) from the APTS were shown from the first to the fifth IMF.

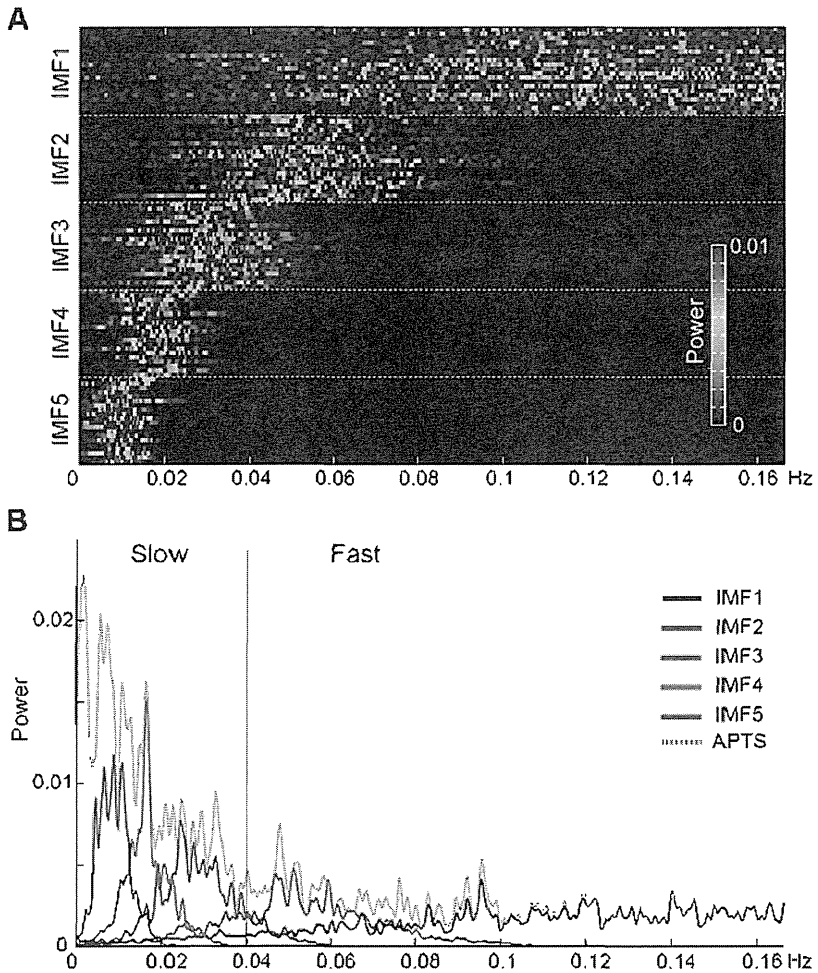

Figure 2. Averaged power spectrums of the IMFs during 20 minutes of fMRI scanning. A: Distribution of the frequency of all IMFs for each subject. Color illustrates the power of the IMFs from 0–0.01. Each line within IMFs represents the frequency spectrum of each subject (total of 20 subjects). B: The averaged power spectrum of the APTS and the IMFs across all subjects. The dashed line represents the averaged power spectrum of the detrended APTS across all subjects. The colors of the profiles represent the spectrum of each IMF as follows. IMF1: blue, IMF2: green, IMF3: red, IMF4: cyan, IMF5: violet. Slow and Fast indicate the frequency ranges of the slow and fast fluctuation components, respectively. 0.04 Hz was the border of the segmentation.

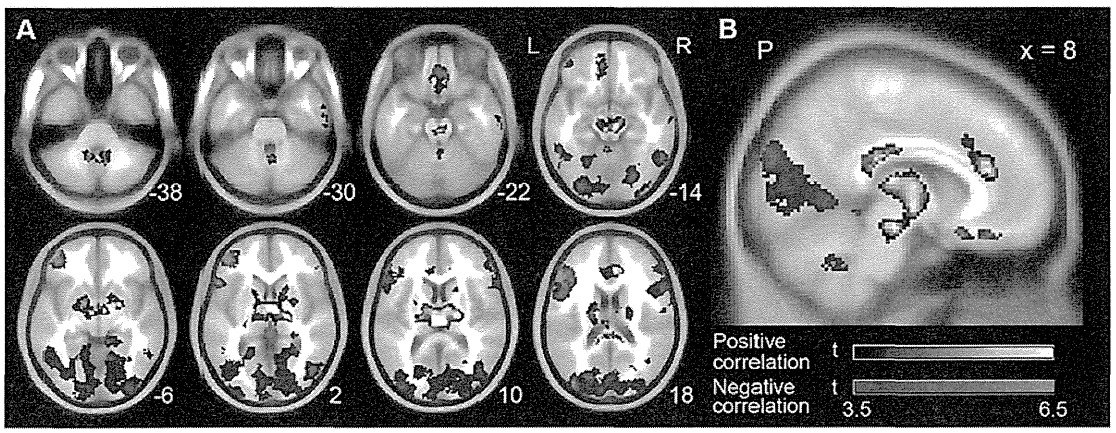

Figure 3. Group analysis of the correlations between alpha power fluctuation and the BOLD signal on fMRI. *A*: The positive (red-white) and negative (blue-green) correlation maps in the multiple axial planes are superimposed on a standard brain template according to the Montreal Neurological Institute (MNI) coordinate [61]. The number in the bottom right of each slice indicates a Z coordinate in the MNI space. *B*: The positive and negative correlation maps in the sagittal planes at an X coordinate of +8 mm in the MNI coordinate. Only the areas with a peak-level uncorrected $p < 0.001$ and a cluster-level FWE of 0.05 by random-effect analysis are shown. The color bars show t-values between 3.5 and 6.5. The letters in the figure indicate the direction of each brain image (L: left; R: right; P: posterior).

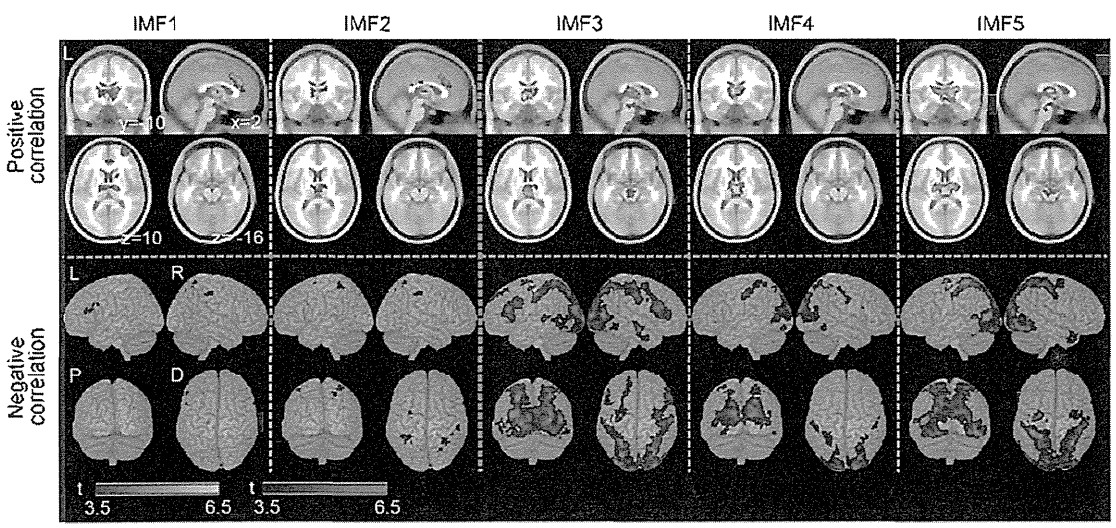

Figure 4. Group analysis of the correlations between IMFs and the BOLD signal on fMRI. In the upper panel, the positive (red-yellow) correlation maps in the multiple axial planes are superimposed on a standard brain template according to the Montreal Neurological Institute (MNI) coordinate [61]. The positive correlation maps for each IMF are shown in the sagittal planes at an X coordinate of +2 mm, a Y coordinate of -10 mm, and a Z coordinate of 10 mm and -16 mm in the MNI coordinate. In the bottom

panel, the negative (blue-green) correlation maps for each IMF are rendered on a standard template brain image. Only the areas with a peak-level uncorrected $p < 0.001$ and a cluster-level FWE of 0.05 by random-effect analysis are shown. The color bars show t-values between 3.5 and 6.5. The letters in the figure indicate the direction of each brain image (L: left; R: right; P: posterior; D: dorsal).

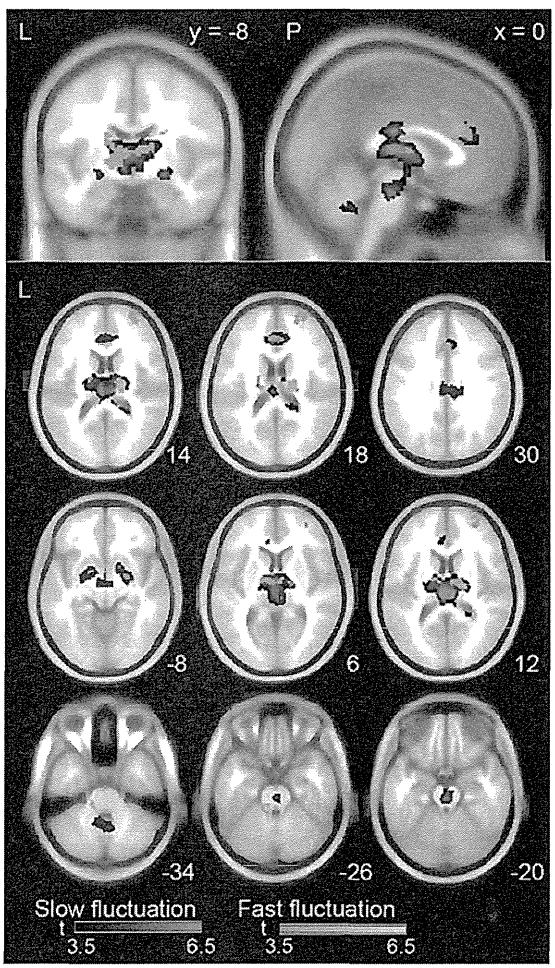

Figure 5. Positive correlation maps between the slow and fast fluctuation of the APTS and the BOLD signal. Only the areas with a peak-level uncorrected $p < 0.001$ and a cluster-level FWE of 0.05 are shown in the random-effect analysis. Statistical results are superimposed on an averaged MRI. The green and orange colors on the brain images indicate the correlation between the BOLD signals and the slow and fast fluctuation components, respectively. The color bars at the bottom of the figure show t-values between 3.5 and 6.5. Numbers in the bottom right of each slice show the coordinates according to the MNI space. Upper: Sagittal and coronal planes. Lower: Multiple axial planes. The letters in the figure indicate the direction of each brain image (L: left; P: posterior).

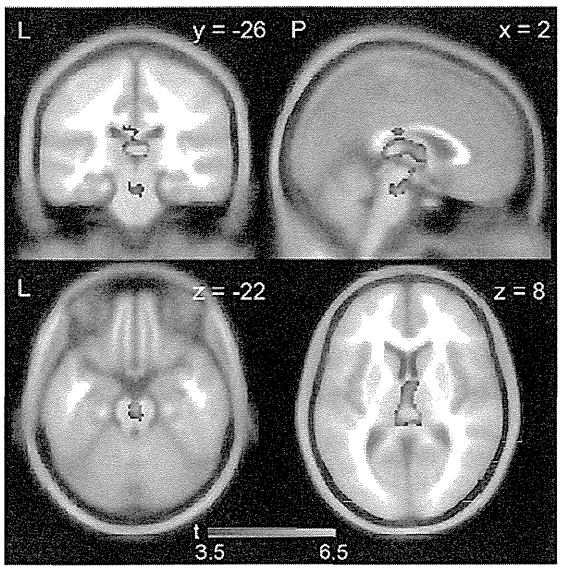

Figure 6. Comparison between the brain regions positively correlated with the slow and fast fluctuation components. Statistical results are superimposed on an averaged MRI (Uncorrected $p < 0.001$, a cluster level FWE of 0.05). The yellow-red color on the brain images indicates the significant difference between the slow and fast fluctuation components (slow > fast). The color bars at the bottom of the figure show t-values between 3.5 and 6.5. The number in the upper right of each slice indicates a MNI coordinate. The letters in the figure indicate the direction of each brain image (L: left; R: right; P: posterior).

Tables

Table 1. Brain regions whose activity correlated with the power of the EEG alpha rhythm (*p*-value, cluster-level FWE of 0.05).

Correlation	Brain region	Side	Local maximum point					
			t-value	X	Y	Z	P value	Cluster size
positive	brainstem	-	9.65	4	-26	-18	< 0.001	4136
	thalamus	bilateral	7.47	-2	-22	10	< 0.001	
			7.07	2	-6	2	< 0.001	
	anterior cingulate cortex	bilateral	6.36	4	34	22	< 0.001	686
	cerebellum	left	5.65	-10	-54	-40	< 0.001	395
	cerebellar vermis	right	5.34	4	-56	-32	< 0.001	
negative	superior parietal lobule, cuneus, middle occipital gyrus	bilateral	7.94	34	-50	56	< 0.001	28926
	middle frontal gyrus	left	7.32	-44	46	0	< 0.001	
	rectal gyrus	bilateral	6.46	-12	44	-16	<0.001	608
	middle frontal gyrus	right	5.68	24	30	44	0.001	211
	Inferior temporal gyrus	bilateral	5.52	56	-54	-12	<0.001	299
	Inferior temporal gyrus	right	5.19	62	-12	-26	<0.001	162

Table 2. Brain regions whose activity positively correlated with the IMFs components of the EEG alpha power (p-value, cluster-level FWE of 0.05).

IMF components	Brain region	Side	Local maximum point					
			t-value	X	Y	Z	P-value	Cluster size
IMF1	thalamus	bilateral	6.31	20	-14	14	<0.001	1159
	anterior cingulate cortex	bilateral	6.24	4	34	26	<0.001	1007
	dorsolateral prefrontal cortex	right	6.07	28	60	14	<0.001	519
	cerebellum	left	5.69	-36	-58	-38	0.001	202
	caudate nucleus	right	4.68	20	12	14	0.032	106
IMF2	anterior cingulate cortex	bilateral	5.47	2	18	36	<0.001	543
	thalamus	left	4.90	-8	-10	0	<0.001	382
		right	4.75	6	-12	10		
IMF3	thalamus	left	6.47	-6	-10	0	<0.001	1332
		right	6.14	4	-12	0		
	brain stem	-	4.82	2	-24	-16		
IMF4	thalamus	bilateral	7.46	-4	-12	12	<0.001	1248
		left	7.32	-4	-4	4		
IMF5	thalamus	bilateral	7.20	0	-20	10	<0.001	2513
		left	6.68	-22	-16	10		
	brain stem	-	5.43	4	-28	-26		
	cerebellum	left	5.66	-28	-70	-32	0.003	225
	supramarginal gyrus	right	5.00	56	-38	42	0.014	171

Table 3. Brain regions whose activity negatively correlated with the IMFs components of the EEG alpha power (p-value, cluster-level FWE of 0.05).

IMF components	Brain region	Side	Local maximum point					
			t-value	X	Y	Z	P-value	Cluster size
IMF1	inferior frontal cortex	left	4.73	-52	24	18	0.011	132
IMF2	superior parietal lobe	left	6.07	-38	-48	58	<0.001	320
		right	5.05	48	-30	42	<0.001	555
	precentral gyrus	right	5.57	30	-2	48	0.032	145
		left	4.78	-28	-6	52	0.004	222
IMF3	occipitoparietal cortex	right	10.35	30	-60	32	<0.001	31596
	inferior frontal cortex	left	7.14	-46	4	30	<0.001	1937
	orbitofrontal cortex	left	6.70	-12	50	-10	<0.001	441
	middle temporal gyrus	right	6.11	64	-12	-16	<0.001	300
IMF4	occipito-parietal cortex	right	7.73	22	-86	18	<0.001	11545
	inferior temporal gyrus	right	6.30	52	-50	-10	0.006	266
	inferior frontal gyrus	right	5.16	46	10	22	0.036	180
IMF5	middle occipital gyrus	left	9.43	-44	-76	6	<0.001	17145
	precentral gyrus	right	7.73	-40	-14	58	<0.001	433
	medial temporal pole	right	5.62	46	12	-40	0.002	253
	middle orbital gyrus	bilateral	5.14	-4	54	-10	0.041	134

Table 4. Brain regions whose activity correlated with the slow and fast fluctuation components of the EEG alpha power and the comparison between the slow and fast fluctuation components (p-value, cluster-level FWE of 0.05).

Fluctuation component	Brain region	Side	Local maximum point					
			t -value	X	Y	Z	P-value	Cluster size
slow	thalamus	bilateral	7.58	6	-24	10	<0.001	2861
	brainstem	bilateral	5.69	0	-22	-22		
	anterior cingulate cortex	bilateral	7.29	6	32	20	<0.001	658
	amygdala	right	7.18	24	-4	-8	0.004	258
		left	7.09	-16	0	-8	0.004	261
	cerebellum	bilateral	5.38	-10	-54	-36	0.006	241
fast	cerebellum	left	7.51	-10	-38	-26	0.024	134
	anterior and middle cingulate cortex	bilateral	5.95	6	18	38	<0.001	489
	superior frontal cortex	right	5.37	28	54	24	0.002	222
	thalamus	right	5.07	18	-16	16	<0.001	487
		left	4.67	-12	-8	0		
slow > fast	thalamus	bilateral	7.97	4	-26	8	<0.001	848
			5.35	-4	-10	-8		
	brainstem	bilateral	5.79	2	-20	-22	0.045	139

乗り物内の音環境を快適化する新しい技術
—ハイパーソニック・エフェクトのアプリケーション—

New technology toward improving the acoustic environment of passenger railway cars
—An application of the hypersonic effect

小野寺英子/東日本旅客鉄道㈱・総合研究大学院大学, 仁科エミ/総合研究大学院大学, 中川剛志/東日本旅客鉄道㈱, 八木玲子/東京成徳短期大学, 福島亜理子/放送大学, 本田学/国立精神・神経医療研究センター, 河合徳枝/国際科学振興財団・早稲田大学, 大橋力/国際科学振興財団
Onodera Eiko[1]/ East Japan Railway Company, SOKENDAI, Nishina Emi[2]/ SOKENDAI, Nakagawa Takeshi[3]/ East Japan Railway Company, Yagi Reiko[4] / Tokyo Seitoku College, Fukushima Ariko[5]/ The Open University of Japan, Honda Manabu[6]/ National Institute of Neuroscience, Kawai Norie[7]/ Foundation for Advancement of International Science, Waseda University, Oohashi Tsutomu[8]/ Foundation for Advancement of International Science
*1 e-onodera@jreast.co.jp , *2 nishina@ouj.ac.jp, *3 t-nakagawa@jreast.co.jp , *4 yagi@tsc.ac.jp , *5 a.fukushima@ouj.ac.jp, *6 honda@ncnp.go.jp , *7 nkawai@fais.or.jp , *8 oohashi@aqua.nifty.jp

Abstract: To address complaints about irritating sounds inside railway passenger cars, we focused on the fact that hypersonic effect, namely the positive effects produced by sounds containing complex high frequency components (HFCs) above the audible range on human physiology and psychology through the activation of the fundamental brain, can induce the positive acceptance of the sound, and applied the hypersonic effect to the improvement of car-interior acoustic environments whose noise level was beyond the limitation of conventional noise reduction approaches. We created a virtual car-interior acoustic environment inside a stable railway car simulator with high fidelity. We obtained HFCs from a rainforest environment where we had confirmed the induction of the hypersonic effect and made it so that it can be added to car-interior acoustic environments. We also developed a hypersonic public announcement containing the HFCs. We evaluated the psychological and physiological effects of the presentation of hypersonic contents simultaneously played alongside a virtual car-interior acoustic environment simulated in a testing car under several conditions. Subjects showed a significantly greater alpha 2-electroenchephalography potential in hypersonic conditions, suggesting an increase in the activation of the fundamental brain. Subjects also showed a significantly more positive impression of the sounds. These findings confirmed the emergence of the hypersonic effect and suggested the more positive acceptance of the car-interior acoustic environments with HFCs than those without HFCs that have identical audible components. The results demonstrate the validity of our approach, that is, by manipulating the sound sensitivity, we can improve the pleasantness of the environments. Our research supports the efficacy of this novel technique in ameliorating the unpleasantness of a noisy environment inside a railway car by means of media content technology.

Keywords: railway cars, hypersonic effect, high-frequency components

1. Introduction

The interior of a railway car is teeming with a cacophony of sounds originating from train itself, the rail lines and machinery parts and from the passengers. Passengers cannot avoid being bombarded by such noises, especially in Japan, where public announcements are customary on trains to notify passengers of the destination. The cars are thus filled with a mishmash of discordant sounds that generate an acoustic environment unpleasant for the passengers.

Previously, the major factor causing the unpleasant auditory sensations in the railway car is thought to be due to the high level of discordant sounds. Therefore, in order to physically reduce noise levels, various attempts have been made including suppression of the source of the sound and by reducing sound transfer from outside by insulation or absorption [Kitagawa et al., 2012).

However, other factors also contribute to the unpleasantness of the acoustic environment— physical factors of sound itself such as its noise level, frequency structure, and duration as well as social factors depending on the public nature or necessity of the sounds, health condition of the passengers, their individual taste or sensitivity to a sound based on past experience of the passengers [Yamamoto et al., 1990].

People have conflicting responses to public announcements played through speaker devices inside a moving train; it seems loud and noisy to some, yet low and inaudible to others. The announcements must be clear enough to be heard by all under extremely noisy conditions, while at the same time it has to be received by the passengers without seeming unpleasant or excessively loud.

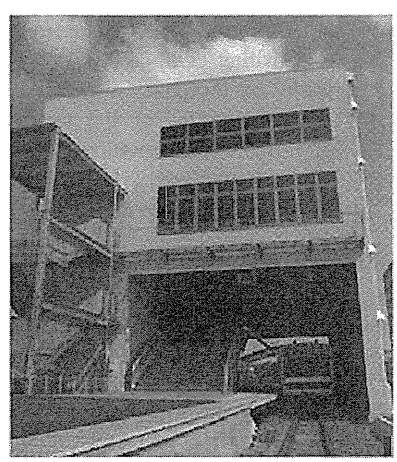

Figure 1: "Smart Station Lab" in Research & Development Center of East JR Group.

The "hypersonic effect" has attracted attention as a possible measure by which to mitigate this complex noise issue. The hypersonic effect is a phenomenon by which non-stationary sounds containing a wealth of inaudible high frequency components (HFCs) above the human audible range, namely hypersonic sound, activate the fundamental brain, which is made up of the midbrain and diencephalon and neural projections from these areas to other parts of the brain, and evoke various positive physiological, psychological, and behavioral responses [Oohashi et al. 2000, 2013].

It has been reported that the hypersonic effect induce a psychological response rendering sounds more pleasant for listeners [Oohashi et al. 1991, 2000], improve the acuteness of the sensitivity [Nishina et al., 2010], and improve the cognitive function [Suzuki, 2013], which is bring about through the activation of the fundamental brain network. Therefore, if the hypersonic effect can modulate the state of the brain of the person hearing the sounds and improve the pleasant acceptance and acuteness of the sounds, it can be a possible breakthrough in improving car-interior acoustic environments whose noise level was beyond the limitation of conventional noise reduction approaches. This hypersonic sound also induces a positive behavioral response, that is, the listener adjusts to a Comfortable Listening Level (CLL) of sounds of a greater magnitude [Yagi et al., 2003].

Further more, many physiological effects have been reported such as an increase in regional cerebral blood flow of the midbrain and the diencephalon [Oohashi et al., 2000], an increase in alpha electroencephalogram (EEG) which is an index of pleasantness [Oohashi et al., 1991, 2000], reduced concentration of the stress hormone adrenaline, and activation of NK cells [Nishina et al., 2005]. These results suggest that hypersonic sounds also have positive effect on physical health, which is additional effect expected in addition to the improvement of car-interior acoustic environments.

Since this effect is based on the physiological activation of the reward-generating system in the fundamental brain network by the presentation of HFCs, it is likely to be universal and unlikely to depend on interests or preferences of individuals, thus making hypersonic sound suitable for the improvement of public acoustic environments. In fact, successful urban environmental designs have succeeded in ameliorating the urban acoustic environment with hypersonic sound [Nishina et al., 2007]. We have already demonstrated significant increase in alpha 2 potential of EEG related to the activation of the fundamental brain network and a more pleasant acceptance of sound by adding inaudible HFCs extracted from hypersonic sound to the station platform acoustic environment [Onodera et al., 2012, 2013].

Therefore, we executed experiments to confirm that, by inducing hypersonic effect to passengers and activating the reward system in their brain, we can improve the acceptance of the identical sounds, and thus can contribute to the improvement of car-interior acoustic environments.

However, it is unrealistic to test this effect on passengers in an actual moving train due to difficulties in coping with passengers to precisely control experimental conditions and so on. Therefore, we employed an East Japan Railway Company (JR East) testing train. This car simulator is in "Smart Station Lab" in Research & Development Center of JR East Group (Figures 1, 2). The simulator is stable and therefore there is no change in the audio-visual environment and no vibrations are noticeable inside the railway car, moreover, it is not necessary for the simulator to run the route on a predetermined timetable carrying a large number of unspecified passengers, experiments can be easily controlled and reproduced.

We decided to test the improvement of the acoustic environment using this simulator by setting up a highly realistic, virtual car-interior acoustic environment. We designed a reproduction system for such an environment. We created a "hypersonic shower" of inaudible HFCs, samples of which were obtained from a tropical rainforest environment in which we had previously confirmed the induction of the hypersonic effect. We also developed a hypersonic public announcement sound by adding the above hypersonic shower to existing public announcements. The system reproduced these high frequency sounds with high fidelity in the simulator.

Using these sound materials and reproduction system, we ran experiments in which we presented complex HFCs extracted from hypersonic sound simultaneously with the virtual car-interior sound. In this paper, we will describe the results of these experiments.

2. Method

2.1. How to produce a virtual acoustic environment in a moving train

2.1.1. Ultra wide-range recording of sounds in a moving train

The usual simple way of dealing with audible sound alone is not appropriate for a virtual reproduction of a moving car-interior acoustic environment in a railway passenger car simulator. It is necessary to record sounds with high fidelity in an ultra wide range in an actual moving train, then reproduce the acoustic environment with high fidelity and reality using the recorded material.

First, it was necessary to record sound in the moving train at an extremely high level of actuality. The frequency response characteristics had to be flat over an extremely

Figure 2: The railway car simulator in "Smart Sation Lab".

high range of up to 100 kHz, which is well beyond the upper limit of the human audible range. It was necessary to have digital recordings of two channels or more with low noise level and high actuality. If we were to smoothly make recordings in a train actually moving with many passengers on board, the system, in addition to meeting the above specifications, had to be small, light, portable and operated by a small staff. It also had to have a DC battery with a long running time so that there would be no AC power cables.

We constructed a recording system that satisfied the above-mentioned strict specifications. We employed a small multi-track PCM recorder (SX-R4, SONOSAX, Switzerland) having 4 channels with a sampling frequency of 192 kHz and quantization of 24 bits. The system weighed 800g and was battery-operated. We selected a small, light, portable non-directional compact condenser microphone (4033, DPA, Denmark) that had frequency characteristics well over 20 kHz, which is known as the upper limit of the human audible range.

Using this recording system, we recorded the environmental sounds in a moving train going out of Tokyo, which had relatively longer intervals between stations, in the evening on a typical weekday. To record the sounds inside the railway car running at high-speed, we made a new microphone arrangement using four microphones; each microphone was directed front, rear, left, and right relative to the direction in which the train was moving. We also measured the equivalent continuous A-weighted sound pressure level with a battery-operated compact integral sound-level meter (LA-5111, Onosokki, Kanagawa, Japan) during recording time, and used that measurement as a reference when we reproduced the acoustic environment for the experiments.

2.1.2 Editing of sound material to reproduce the acoustic environment in a moving passenger train

We created sound material to reproduce acoustic environments using the car-interior environment recordings. Using a digital audio workstation (PCM8, SADiE, UK), we removed unexpected noises and public announcements that may interfere with the experiment, and created a 24-minute sound material. We then input these 4 channels signals into a mixing console (9098i, AMEK, UK) that has a super-wide bandwidth. Using the surround editing function of the console, we edited the virtual car-interior acoustic environment so that sounds originally recorded in the front, rear, left, and right microphone in the direction the train was running were localized to correspond to the arrangement of the speakers, which were set in the front left, front right, rear left, and rear right.

The public announcement was removed from the car-interior environment recordings. In its stead, an actual public announcement made by a female speaker that had been used in a railway car was converted to a format with a sampling frequency of 192 kHz and quantization of 24 bits by means of a SADiE audio workstation. Since the upper limit of the frequency included in the announcement did not exceed 22.05 kHz even after format conversion, we call these sounds a "high-cut announcement". The combined replay of the virtual car-interior acoustic environment and the high-cut announcement virtually realized the acoustic environment of a moving passenger train.

2.1.3. Reproduction system of sound materials

During the experiment, subjects sat in two rows of seats facing each other in the room in which the sound reproduction system for the virtual car-interior acoustic environment was set up. Virtual car-interior environmental sounds were presented in the railway car simulator through four full-range speakers (PS-10, NEXO, France), each of which corresponded to one of the four channels. Taking into consideration the rich lower frequency components in the car-interior acoustic environment, we added two subwoofers (System5000, APOGEE, USA) to reproduce the low frequency sounds. For the presentation of the control high-cut announcement, we used originally developed full-range speakers (OOHASHI Monitors Op.5) that could also reproduce HFCs, as described below.

Using this sound reproduction system, the virtual car-interior sound was reproduced in the experimental space in which subjects felt as though they were actually seated in a moving railway car (Figure 3).

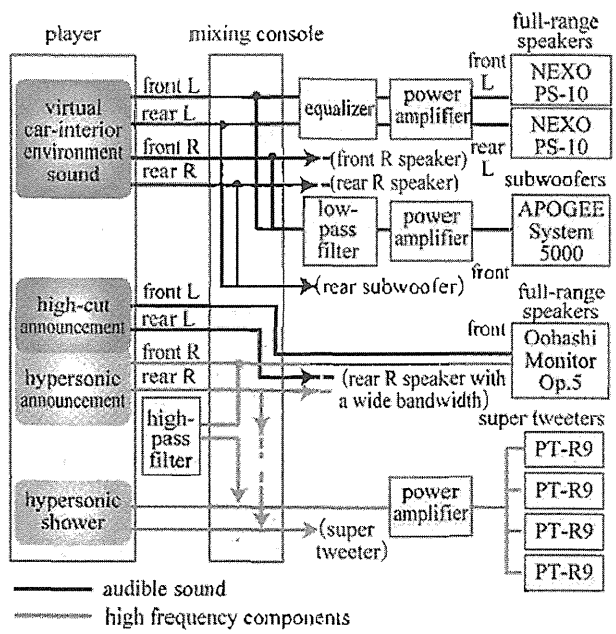

Figure 3: Sound presentation system.

2.2. How hypersonic sound was added and presented

2.2.1. Creating of 'hypersonic shower' and 'hypersonic announcement'

The hypersonic sound used in this experiment, as in previous research, had to be rich in complex HFCs that would be sure to increase the cerebral blood flow in the fundamental brain. In addition, the safety of the sound had to be guaranteed. A sound source that satisfied these conditions was found, in a previous study, in a tropical rainforest. High fidelity recordings of natural environment

sounds of a rainforest, where human genes evolutionarily developed, were reported to increase the alpha 2 EEG potential [Nishina et al., 2007]. Therefore, in this experiment, we used the environmental sounds of a tropical rainforest recorded with a sampling frequency of 5.6448 MHz and quantization of 1 bit. From this sound that included frequencies over 100 kHz, we extracted HFCs above the human audible range using an analog high-pass filter with a cutoff frequency of 20 kHz (-80dB/oct), and recorded with a sampling frequency of 192 kHz and quantization of 24 bit. We called these extracted components a hypersonic shower. We excluded the audible contents to eliminate the effect of individual preferences for sounds and to avoid adding audible sounds to an already extremely noisy car-interior environment.

We then mixed a high-cut announcement with this hypersonic shower correlating it with the sound pressure level of the announcement. We called this mixed sound a hypersonic announcement.

2.2.2. Sound presentation system

Speakers should have favourable frequency characteristics over a wide range and be small enough to minimize the visual feeling of pressure to reproduce the hypersonic shower and hypersonic announcement. We used super tweeters (PT-R9, Pioneer, Japan) to present the hypersonic shower in the acoustic environment. For the presentation of the hypersonic announcement, we used full-range OOHASHI Monitors Op.5 speakers and PT-R9 super tweeters. We presented the hypersonic announcement and the high-cut announcement with identical speakers (Figure 3).

2.3. Experimental condition and design

Using the sound material and presentation system described above, we set up the following three experimental conditions: full-hypersonic condition in which the virtual car-interior sound, hypersonic announcement and hypersonic shower were presented simultaneously; hypersonic shower condition in which the virtual car-interior sound, high-cut announcement and hypersonic shower were presented simultaneously; and control condition in which the virtual car-interior sound and the high-cut announcement were presented simultaneously (Table 1).

Figure 4 shows the frequency power spectrum of the electric signals of sound material for the virtual car-interior sound (the upper panel) and that of the reproduced sounds measured by microphone (the lower panel) (4939, Brüel & Kjær, Denmark) located near the subjects. We analyzed the data with an FFT analyzer (CF-5220, Onosokki, Kanagawa, Japan).

Table 1: Three experimental conditions and sound material.

condition		sound material	
full-hypersonic condition	virtual car-interior sound	hypersonic announcement	hypersonic shower
hypersonic shower condition	virtual car-interior sound	high-cut announcement	hypersonic shower
control condition	virtual car-interior sound	high-cut announceme	

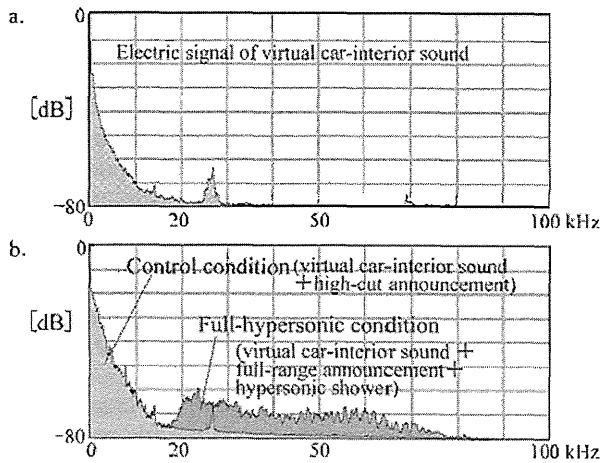

Figure 4: Frequency power spectrum of the electric signals and the reproduced sound.

The power of the sound recorded inside the moving train showed prominent audible components below 20 kHz but its upper limit occasionally and instantaneously reached over 20 kHz. The configuration of the spectrum of the electric signals and replayed sound of car-interior sound and hypersonic sound at the subject's location agree well with each other, suggesting the car-interior sounds was reproduced with high fidelity. In the full-hypersonic and hypersonic shower conditions, sounds up to almost 80 kHz were confirmed to reach the subjects.

Using these experimental conditions, we performed five experiments as follows:

Experiment 1: Investigation of the effect of a full hypersonic condition
Experiment 2: Investigation of the effect of a hypersonic shower condition
Experiment 3: Investigation of the duration of the hypersonic sound presentation
Experiment 4: Examination of the effect of the order of sound presentation
Experiment 5: Hypersonic effect on earphone-wearers

The duration of the sound presentations differed across experiments, but never exceeded 21 minutes.

2.4. Physiological evaluation

For the physiological evaluation of the hypersonic effect, we measured the alpha 2 frequency component (10–13 Hz) of a spontaneous EEG potential which has been shown to correlate with the cerebral blood flow of activity in the fundamental brain region through simultaneous measurement of Positron Emission Tomography and EEG [Oohashi et al., 2000].

We measured spontaneous EEGs of the subjects during the presentation of the sounds by the use of a telemetry EEG measurement system, which had less movement restriction

(EEG-9100 and WEE-1000, Nihon-Kohden, Tokyo, Japan, and Synact MT-11, NEC Corporation, Tokyo, Japan, and originally developed wearable EEG system supported by JST-CREST, Kawaguchi, Japan). We used EEG caps with all the electrodes sewn on beforchand in the international 10-20 system arrangement.

Sixteen healthy subjects with normal hearing ability (nine males and seven females, ranging in age from 34 to 62) participated in one or more of the five experiments. None of the subjects had any history of neurological or psychiatric disorders. Written informed consent was obtained from each of them before the experiments. The experiments were performed in accordance with the approval of the Ethics Committee, National Center of Neurology and Psychiatry. Subjects, however, were not informed of the specific purpose or conditions of the experiments in which they participated. Subjects were asked to sit in a relaxed manner on the seat in the simulator car with their eyes closed.

To detect the difference between the sound containing HFCs, namely, the full hypersonic and the hypersonic shower conditions, and that without HFCs, namely the control condition, subjects were first presented with the control condition, and then with either the full-hypersonic or the hypersonic shower condition. Background to the presentation order is noted below. Previous studies have shown that an increase in alpha power caused by the hypersonic effect is delayed by tens of seconds after the onset of the hypersonic sound, and remains until about 100 seconds after the termination of the hypersonic sound [Oohashi et al., 1991]. Therefore, if the presentation is short and the hypersonic condition is presented first, the effect of the full-hypersonic or hypersonic shower condition may remain and overlap with the effect of the control condition following it. Therefore, in the present study, we employed a relatively long presentation of at least 12 minutes, and the control condition without HFCs was always presented first for all the subjects.

The power spectrum of the EEG at each electrode was calculated using FFT analysis, and the square root of the averaged power level in a frequency range of 10.0-13.0 Hz at each electrode position was calculated as the equivalent potential of EEGs in the alpha 2 band. To eliminate inter-subject variability, the EEG data were normalized with respect to the mean value across all time epochs and conditions for each subject. After excluding epochs contaminated by artifacts, the data obtained from 7 electrodes in the centro-parieto-occipital region were averaged and compared between the two conditions. Paired Student's t-test between 2 conditions was performed for statistical evaluation.

2.5. Psychological evaluation

All subjects taking part in the psychological experiments also participated in the physiological experiments. In each experiment (Experiment 1, 2 and 5) we first presented a control condition, then a full-hypersonic or a hypersonic shower condition and finally the control condition again to confirm the initial impression. Each presentation was two minutes in duration.

After the presentation of each sound, the subjects marked their reaction to the presented sounds on a five-step scale questionnaire. It consisted of five items evaluating the announcement in the railway car, two items evaluating the sound of the moving train, six items evaluating their overall impression of the acoustic environment. In Experiment 5, two items evaluating the music heard through earphones were added to the above 13 items. There was an interval between the conditions to give the subjects enough time to fill out the questionnaire (Table 2). The results were tested using the Wilcoxon signed rank sum test.

Table 2: Construction of the questionnaire

Words for evaluation (negative—positive)		
about announcement in railway car		
The public announcement was noisy	–	The public announcement was not noisy
The public announcement was difficult to hear	–	The public announcement was easy to hear
The voice of the public announcement was not pleasant	–	The voice of the public announcement was pleasant
The public announcement sounded cold and mechanical	–	The public announcement sounded warm and human
The public announcement was nervous	–	The public announcement was calm
about sound of the moving train		
The sound inside the train was noisy	–	The sound inside the train was not noisy
The sound inside the train was unpleasant	–	The sound inside the train was unexpectedly pleasant
about overall impression		
The sound made me irritated	–	The sound did not make me irritated
The atmosphere was unpleasant	–	The atmosphere was not unpleasant
I was feeling tired	–	I was not feeling tired
The sound was not clear	–	The sound was clear
I was annoyed	–	I was not annoyed
Unable to listen to the sound for a long time (not bearable)	–	Able to listen to the sound to some degree (bearable)
about music from earphone		
Music from earphone sounded worse than usual	–	Music from earphone sounded better than usual
Music from earphone was difficult to hear	–	Music from earphone was easy to hear

3. Result

3.1. Experiment 1: Investigation of the effect of a full hypersonic condition

3.1.1. Overview

In our first experiment, we investigated whether the hypersonic effect would emerge in a full-hypersonic condition in which both the hypersonic announcement and hypersonic shower were presented in a railway car. For this experiment, we designed and compared two conditions: a full-hypersonic condition in which virtual environmental sounds in a railway train, a hypersonic announcement and a hypersonic shower were presented, and a control condition in which virtual environmental sounds in a railway train and a high-cut announcement were presented. Fourteen subjects with normal hearing ability (eight males and six females, ranging in age from 34 to 62) participated in the physiological experiment, and sixteen subjects (nine males and seven females, ranging in age from 34 to 62) participated in the psychological experiment.

3.1.2. Results of the physiological experiment

Increase in alpha 2 EEG potential was greater in the full-hypersonic condition than in the control condition with a high statistical significance of $p = 0.006$ (Figure 5), which indicates activation of the fundamental brain of the subjects through the emergence of the hypersonic effect.

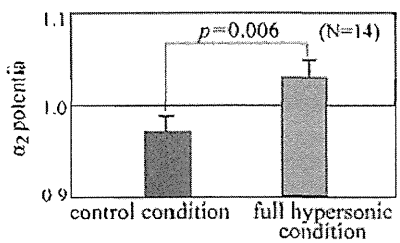

Figure 5: Mean and SD of the increase in alpha 2 potentials under two conditions in Experiment 1.

3.1.3 Results of the psychological experiment

The subjects reacted negatively to twelve of the 13 items on the questionnaire in the control condition. In contrast, reaction to twelve of them was positive in the full-hypersonic condition. That is to say, as many as eleven of the thirteen items indicated that full-hypersonic condition brought less unpleasant and more positive feelings than the control condition with statistical significance (Figure 6). The items that showed statistical significance were "the public announcement was not noisy" ($p < 0.01$), "the public announcement was easy to hear" ($p < 0.05$, same value hereinafter), "the voice of the public announcement was pleasant", "The public announcement sounded warm and human", "the sound inside the train was not noisy", "the sound inside the train was unexpectedly pleasant", "the sound did not make me irritated", "the atmosphere was not unpleasant", "the sound was clear", "I was not annoyed" and "I was able to listen to the sound to some degree".

As observed above, we found that the addition of hypersonic sounds to a car-interior acoustic environment caused a hypersonic effect in the fundamental brain of the subjects resulting in a more pleasant feeling about the car-interior acoustic environment (Figure 6).

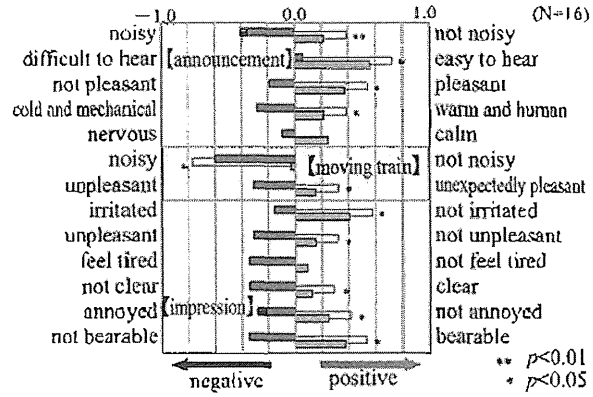

Figure 6: Mean score of each item in the questionnaire in Experiment 1.

3.2. Experiment 2: Investigation of the effect of a hypersonic shower condition

3.2.1. Overview

Public announcements vary according to the railway line, so it would be too costly in terms of time and money to convert all of them into hypersonic announcements. On the contrary, if we could bring about the hypersonic effect just by adding only HFCs to car-interior acoustic environment, the general application of the effect would be enhanced because this would not require customization to individual public announcements and the expense would be greatly reduced. As a result, we conducted a second experiment in which we investigated the effect of the hypersonic shower condition in which only HFCs were added to the acoustic environment. Twelve subjects with normal hearing ability (seven males and five females, ranging in age from 37 to 62) participated in the physiological experiment, and thirteen subjects (seven males and six females, ranging in age from 37 to 62) participated in the psychological experiment.

3.2.2. Results of physiological experiment

Increase in alpha 2 potential was greater for the hypersonic shower condition with a statistical significance of $p < 0.05$ than for the control condition (Figure 7). That is, the

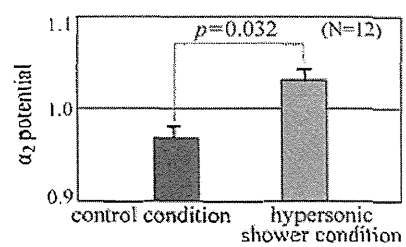

Figure 7: Mean and SD of the increase in alpha 2 potentials under two conditions in Experiment 2.